The response of the southern annular mode, the East Australian Current, and the southern mid-latitude ocean circulation to global warming

W. Cai,[1] G. Shi,[2,1] T. Cowan,[1] D. Bi,[1] and J. Ribbe[2]

Climate models predict an upward trend of the southern annular mode (SAM) in response to increasing atmospheric CO_2 concentration, however the consequential impact of this change on oceanic circulation has not been fully explored. Here we analyse the outputs of a series of global warming experiments from the CSIRO Mark 3 climate model. We show that although for the zonal wind stress change the maximum is located at approximately 60°S, in terms of the change in surface wind stress curl, the maximum is situated at approximately 48°S. This change in the wind stress curl causes a spin-up of the entire southern midlatitude ocean circulation including a southward strengthening of the subtropical gyres, particularly the East Australia Current (EAC). The intensified EAC generates a warming rate in the Tasman Sea that is the greatest in the Southern Hemisphere (SH) with significant implications for sea level rise. The pan-Southern Ocean scale suggests a broad impact on the marine ecosystem of the entire southern midlatitude ocean.

1. Introduction

Over the past several decades, there has been an upward trend of the SAM [*Thompson et al.*, 2000; *Marshall*, 2003; *Marshall et al.*, 2004] with increasing mean sea level pressure (MSLP) in the midlatitudes. The cause of the upward trend is a contentious issue. Observational [*Thompson and Solomon*, 2002] and other modelling studies [*Sexton*, 2001; *Gillett and Thompson*, 2003] indicate that it is attributable to ozone depletion over the past decades. Under increasing atmospheric CO_2, climate models produce an increasing midlatitude MSLP incorporated in an upward trend of the SAM [*Fyfe at al.*, 1999; *Kushner et al.*, 2001; *Cai et al.*, 2003a]. Although the extent to which the increasing CO_2 over the past decades contributes to the observed SAM trend is not clear, as CO_2 continues to increase, a strengthening of the SAM trend is projected into the future. This is one of the most robust and consistent responses of the global climate system to climate change. To date, the focus has been on impacts of the projected SAM trend upon the climate from the stratosphere to Earth's surface, with little attention given to the consequential ocean circulation.

[1]CSIRO Marine and Atmospheric Research, PMB 1, Aspendale, Victoria 3195, Australia. (wenju.cai@csiro.au)
[2]Department of Biological and Physical Sciences, University of Southern Queensland, Toowoomba 4350, Queensland, Australia

0094-8276/05/$5.00

This is the focus of the present paper. We analyzed outputs of an ensemble of four climate change experiments with the CSIRO Mark 3 climate model forced by four different projections. The results show significant ocean circulation changes of pan-Southern Ocean scale.

2. The CSIRO Mark 3 climate model

The "Mark 3" model [*Gordon et al.*, 2002; *Cai et al.*, 2003b] runs without flux adjustments. As in its previous version [*Cai et al.*, 2003a], when subject to climate change forcing [*Cai et al.*, 2003c], the model SAM exhibits an upward trend. Here we focus on a control simulation, and four climate change experiments. The four climate change experiments following the A2 (two experiments), A1B, and B1 scenarios all incorporating CO_2 forcing, direct effect of sulfate aerosols, and ozone depletion. Each of the four experiments starts from a different time of the control experiment, and together they provide an ensemble strategy. The ozone forcing incorporates a full recovery of the ozone content by 2048. Despite this, in all warming experiments the SAM shows an increasing trend. In what follows, we show changes of a 31-year mean over the period of 2055-2085 averaged over the four climate change experiments from a control climate. Although we show only the averaged pattern, each individual experiment produces a change pattern that is similar to the average, highlighting the robustness of the change.

3. Results

Strong zonal wind changes take place (Fig. 1a), with the maximum located at 60°S. Since it is the wind stress curl, not the wind stress itself, that drives ocean circulation, we calculate the change of the wind stress curl, which is dominated by the meridional gradient of changes in zonal wind stress. An important feature is that although the location of the maximum change in zonal wind stress is at approximately 60°S [*Thompson and Solomon*, 2002; *Gillett and Thompson*, 2003], the maximum curl change is located at approximately 48°S (Fig. 1b). Spatially, large increases in the positive wind stress curl are observed south of the Tasman Sea and New Zealand.

Sverdrup balance implies a significant change to the wind driven circulation. At 36°S the zonal average of curl from the east to the west boundary is $1.4 \times 10^{-8} Nm^{-3}$. Sverdrup relationship produces an intensification of the basin interior transport, and an implied EAC transport increase at this latitude of approximately 10 Sv (1 Sv $= 10^6$ m^3 s^{-1}). Changes in the modeled barotropic transport streamfuction (Fig. 1c) confirm a change of this magnitude. Moreover, the strengthening of the EAC is part of a larger scale circulation change: the entire southern midlatitude circulation intensifies with a large change in the South Atlantic Ocean.

To confirm that the wind stress changes are the major forcing of the circulation change, we use Godfrey's Island Rule model [*Godfrey*, 1989] to obtain a depth-integrated transport streamfunction, using wind stress of the control and warming experiments. As Sverdrup circulation requires an eastern boundary, we carry out the calculation to the southern-most latitude, 54°S. The wind stress inputs are interpolated onto a 2×2 degree grid as in the original algorithm, with the Indonesian Throughflow Passage open.

The wind-driven EAC (Figs. 2a and 2b) bifurcates at

approximately 20°S. Part of the EAC separates from the coast at approximately 32°S, the majority passes through the Tasman Sea. The flow then veers northwest into the Great Australian Bight, Indian Ocean, and to the Atlantic Ocean, before it retroflects, forming a southern midlatitude inter-basin "super-gyre," linking the South Pacific, Indian and Atlantic Oceans [*Ridgeway and Dunn*, 2003; *Tilburg et al.*, 2001]. The central features are: first, the South Pacific subtropical gyre increases significantly. This is clearly seen in the difference plot (Fig. 2c); second, the increase in the flow passing through the Tasman Sea is accompanied by stronger recirculations in the longitudes from east of New Zealand to the eastern boundary (the South American coast); finally, the Southern Ocean super-gyre strengthens and shifts southward (Fig. 2c).

There is a strong resemblance between the wind-driven change (Fig. 2c) and the total change from the model output (Fig. 1c) in the midlatitudes. This means that the midlatitude changes in the ocean circulation are primarily driven by the wind changes. Both the coupled model and the Godfrey model predict an annual mean increase of about 10 Sv in the EAC flow passing through the Tasman Sea. In the coupled model, the change is also forced by buoyancy forcing and its interactions with bottom topography. The positive change of the streamfunction in the longitude band of 90°E to 160°E (Fig. 1c), indicating a local change with a strengthening clockwise circulation, is propabably due these processes, as it is not present in the circulation change inferred from the wind (Fig. 2c).

The reason that the EAC increases more markedly than other subtropical gyres is because the southern-most tip of the lateral boundaries of the South Pacific gyre are either close to or extend into the zonal strip of strong curl changes. This feature allows the South Pacific gyre to tap into the effect of the curl changes integrated from the South American coast, through New Zealand, to the East Australian coast. The resultant circulation changes is stronger, broad northward flows in the interior and off New Zealand's northeast coast, and swifter narrow southward EAC flows through the Tasman Sea as a result of Stommel's westward intensification. In the latitude band of 43°-54°S, a similar process takes place; the two sides of the South American continent form the major east and west boundaries. The effect of the strong wind stress curl changes is a narrow but swift flow off the west boundary (Fig. 2c), again via the Stommel's westward intensification process. Consequently, the greatest change occurs off the west boundary of the South Atlantic. Overall, the pattern (Fig. 2c) is consistent with the notion of a southward shift and a spin-up of the mid- to high- latitude Southern Ocean circulation, postulated in previous studies [*Gille*, 2003; *Swift*, 1995].

A direct consequence of the EAC increase is strong warming along the path of the EAC intensification and cooling along the path of increased northward recirculations (Fig. 3). The biggest change is situated at the subsurface, with a baroclinic structure of the EAC response, which includes undercurrents at depth flowing in opposite directions to the surface flows, generating temperature trends of opposing polarities at depth to those closer to the surface. Spatially, it is the strengthening of the EAC that drives the large warming in the Tasman Sea (Fig. 4a) with a warming rate that is greatest in the SH. Changes of heat flux (Fig. 4b) further reinforce the role of the EAC change in generating the large warming in the Tasman Sea. For example, at the center of the Tasman warming, there is a large increase in the heat loss

from the ocean to the atmosphere. This eliminates the possibility of the warming being forced by atmospheric heating.

There is a correspondence between the change pattern of wind stress curl and that of the heat flux. In areas where there is an increase in positive curl, the ocean gains heat, and vice versa. This can be seen in several northwest-southeast orientated strips in the subtropical southern Indian Ocean, as well as in the Tasman Sea, where the strong heat loss is associated with a decrease in the wind stress curl. The correspondence suggests that the change in wind stress curl in fact reflects a series of air-sea couplings in terms of not only the momentum exchange but also the thermal interactions. Examinations reveal that the large warming in the Tasman Sea leads to an increase in out-going longwave radiation from the surface contributing to the ocean heat loss. The warming enhances local convection with increased cloud and rainfall, leading to a reduction in shortwave radiation reaching the surface, hence cooling the ocean. However, the most important processes contributing to the heat loss are warming-induced increases in evaporation and in sensible heat transfer from the ocean to the atmosphere. Thus the large warming takes place despite these cooling mechanisms, highlighting the powerful warming effect of the southward shift of the EAC, and the consistency of the thermal and dynamical response in a fully coupled environment.

4. Conclusions and discussion

We have demonstrated that, in response to climate change forcing, the midlatitude Southern Ocean super-gyre circulation intensifies and shifts southward. The biggest circulation change is near the western boundary of the South Atlantic in the latitude band of 44°-54°S. The circulation change includes a strengthening of the EAC flow through the Tasman Sea. The EAC change is greater than other subtropical gyres and the strengthening EAC generates a warming rate in Tasman Sea that is the largest of the entire SH. Overall, the inter-basin connectivity of the super-gyre is strengthened. Although much of the circulation change is attributable to changes in the atmospheric surface flows, it is interesting that the wind change bears the imprints of the response of the air-sea thermal interactions, which in turn reflects the change in ocean temperature.

Over the past several decades, marine ecosystem of the South Pacific has experienced significant changes, with a range of species extending south [*Eagar*, 1987; *Thresher et al.*, 2003]. This is consistent with a strengthening EAC generated by changes in wind stress curl, which are principally associated with the observed upward trend of the SAM. Our result indicates that these trends and the impact will continue into the future. Further, given the pan-Southern Ocean scale of the circulation change, the impact on the marine ecosystem is likely to be broad in scale, far beyond the South Pacific.

Acknowledgments.
This work is supported by the CSIRO Wealth from Ocean Flagship and the Australian Greenhouse Office. We thank members of the CSIRO Climate Model and Application Team for developing the model and performing the experiments.

References

Cai, W. J., P. H. Whetton, and D. J. Karoly, The response of the Antarctic oscillation to increasing and stabilized atmospheric CO_2. *J. Climate*, *16*, 1525-1538, 2003a.

Cai, W.J., M. A. Collier, H. B. Gordon, and L. J. Waterman, Strong ENSO variability and a super-ENSO pair in the CSIRO coupled climate model. *Mon. Wea. Rev.*, *131*, 1189-1210, 2003b.

Cai, W. J., M. A. Collier, P. J. Durack, H. B. Gordon, A. C. Hirst, S. P. O'Farrell, and P. H. Whetton, The response of climate variability and mean state to climate change: preliminary results from the CSIRO Mark 3 coupled model. *CLIVAR Exchanges, 8(4)*, 8-11,16-17,2003c.

Edgar, G.J., Australian Marine Life, Reed Books, Sydney, 1997.

Fyfe, J. C., G. J. Boer, and G. M. Flato, The Arctic and Antarctic oscillations and their projected changes under global warming, *Geophys. Res. Lett., 26*, 1601–1604, 1999.

Gille, S. T., Warming of the Southern Ocean since the 1950s. *Science*, *295*, 1275-1277, 2002.

Gillet, N. P., and D. W. J. Thompson, Simulation of recent Southern Hemisphere climate change, *Science*, *302*, 273–275, 2003.

Godfrey, J. S., A Sverdrup model of the depth-integrated flow for the world ocean allowing for island circulations. *Geophys. Astrophy. Fluid Dyn.* it 45, 89-112, 1989.

Gordon, H.B., L.D. Rotstayn, J.L. McGregor, M.R. Dix, E.A. Kowalczyk, S.P. O'Farrell, L.J. Waterman, A.C. Hirst, S.G. Wilson, M.A. Collier, I.G. Watterson, and T.I. Elliott, The CSIRO Mk3 Climate System Model, CSIRO Division of Atmospheric Research technical paper No. 60. 130pp, 2002.

Kushner, P. J., I. M. Held, and T. L. Delworth, Southern Hemisphere atmospheric circulation response to global warming. *J. Climate*, *14*, 2238-2249, 2001.

Marshall, G. J., Trends in the Southern Annular Mode from observations and reanalyses, *J. Climate*, *16*, 4134 - 4143, 2003.

Marshall G.J., et al., Causes of exceptional atmospheric circulation changes in the Southern Hemisphere, *Geophys. Res. Lett.*, *31*, L14205, doi: 10.1029/2004GL019952, 2004.

Ridgway, K. R. and J. R. Dunn, Mesoscale structure of the mean East Australian Current system and its relationship with topography, *Prog. Oceanography. 56,* 189-222 2003.

Sexton, D. M. H., The effect of stratospheric ozone depletion on the phase of the Antarctic Oscillation, *Geophys. Res. Lett.*, *28*, 3697-3700, 2001.

Swift, J. H., Comparing WOCE and historical temperatures in the deep southeast Pacific. *International WOCE Newsletter*, *18*, 15-17, 1995.

Thompson, D. W. J., and S. Solomon, Interpretation of recent Southern Hemisphere climate change, *Science*, *296*, 895-899, 2002.

Thompson, D. W. J., J. M. Wallace, and G. C. Hegerl, Annular modes in the extratropical circulation, Part II: Trends. *J. Climate*, *13*, 1018-1036, 2000.

Thresher, et al., Invasion dynamics of the European green crab, Carcinus maenas, in Australia, *Marine Biology*, *142*, 1018-1036, 2003.

Tilburg, C. E., H. E. Hurlburt, J. J. O'Brien, and J. F. Shriver, The dynamics of the East Australia Current system: the Tasman Front, the East Auckland Current, and the East Cape Current, *J. Phys. Oceanogr.*, *13*, 1018-1036, 2001.

Wenju Cai, CSIRO Marine & Atmospheric Research, PMB 1, Aspendale, Victoria 3195, Australia. (wenju.cai@csiro.au)

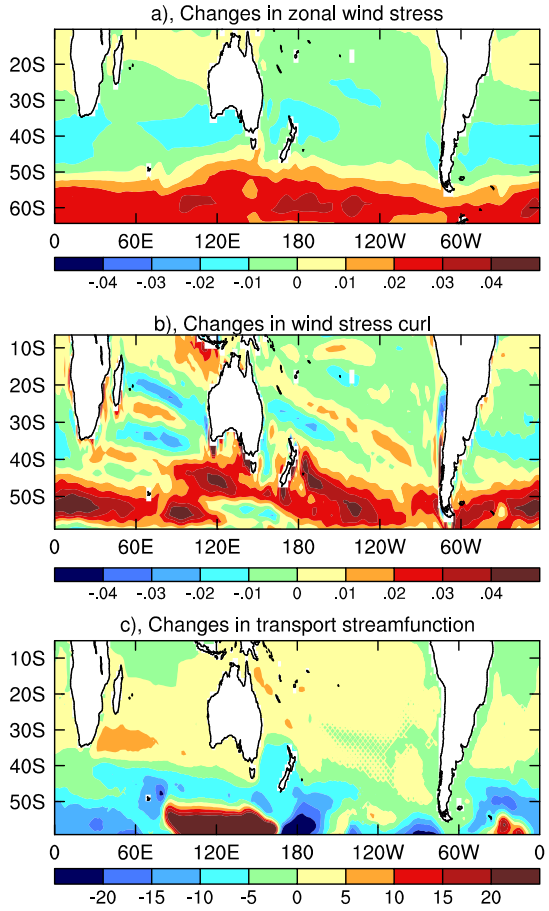

.

Figure 1. Ensemble-mean change averaged over the period of 2055-2085, a) zonal wind stress (N m^{-2}), b) wind stress curl (N m^{-3} scaled by a factor of 10^{-6}), and c) vertically integrated barotropic streamfunction (Sv, $1Sv = 10^6$ m^3 s^{-1}). The pattern correlation coefficients between individual ensemble members are in the range of 0.95-0.98 for a), 0.87-0.95 for b), and 0.93-0.99 for c).

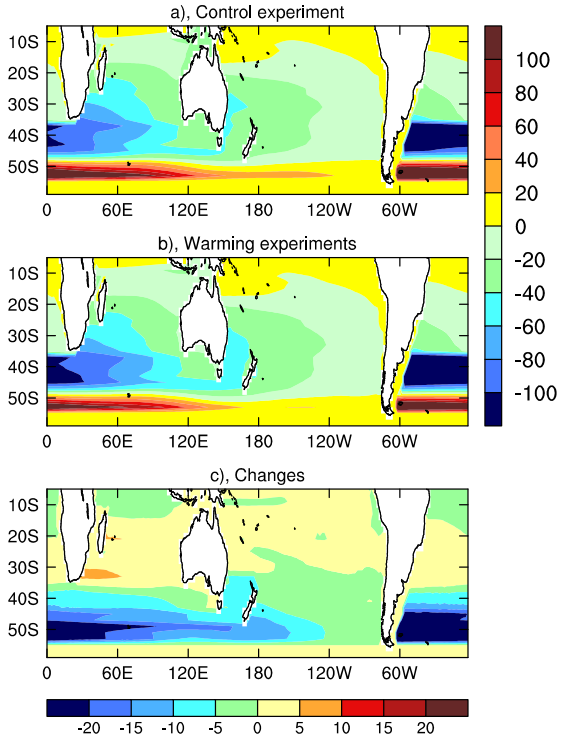

.

Figure 2. Transport streamfunction (Sv) from Godfrey's Island Rule model forced by model winds from, a) control experiment, b) ensemble-mean of warming experiments averaged over 2055-2085, and c) difference between b) and a). The pattern correlation coefficients between individual ensemble members are in the range of 0.95-0.98 for zonal wind stress change and 0.87-0.96 for meridional wind stress change.

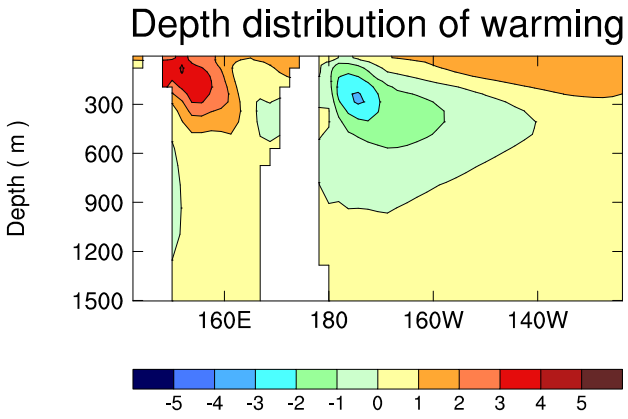

Figure 3. Ensemble-mean changes in temperature (°C) along the 36°S section of the South Pacific. The pattern correlation coefficients between individual ensemble members are in the range of 0.89-0.99.

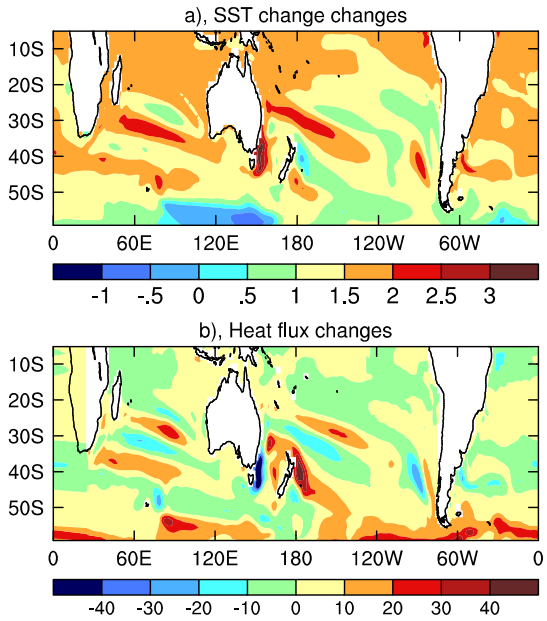

.

Figure 4. a) Ensemble-mean changes in SST (^{o}C). The pattern correlation coefficients between individual ensemble members are in the range of 0.96 - 0.99. b), as in a) but for surface heat flux (W m^{-2}), positive into the ocean. The pattern correlation coefficients between individual ensemble members are in the range of 0.88-0.98.